ELSEVIER

Polymer 41 (2000) 8543–8556

polymer

www.elsevier.nl/locate/polymer

Diffusion and reaction of epoxy and amine in polysulfone-transport modeling and experimental validation

G. Rajagopalan[a], C. Narayanan[b], J.W. Gillespie Jr.[a,c,*], S.H. McKnight[d]

[a]*201 Composite Manufacturing Science Laboratory, Center for Composite Materials and Department of Materials Science and Engineering, University of Delaware, Newark, DE 19716-3144, USA*

[b]*College of Marine Studies, University of Delaware, Newark, DE 19716-3144, USA*

[c]*Department of Civil and Environmental Engineering, University of Delaware, Newark, DE 19716-3144, USA*

[d]*Army Research Laboratory, Materials Directorate, Aberdeen Proving Grounds, MD, USA*

Received 22 September 1999; received in revised form 20 March 2000; accepted 23 March 2000

Abstract

In this work, a mathematical model for the multi-component diffusion of reacting thermosets into amorphous thermoplastics is presented for the epoxy–amine-polysulfone (PSU) system. The governing Fickian diffusion-reaction equations for the epoxy and amine are strongly coupled through the amine concentration dependence of the epoxy diffusivity and the autocatalytic reaction terms for the epoxy and amine. Expressions for epoxy and amine diffusivity were used to formulate the coupled governing equations for the epoxy and amine, and solved numerically using finite difference methods. The model predictions are coupled with experimental Attenuated Total Reflectance-Fourier Transform Infrared Spectroscopy (ATR-FTIR) and Scanning Electron Microscopy-Energy Dispersive Spectroscopy (SEM-EDS) data. It is shown that despite certain simplifying assumptions, relatively good agreement is found for the concentration distributions with time and distance, and the interphase size as a function of processing temperature.

Keywords: Epoxy–amine/polysulfone; Coupled diffusion-reaction-swelling; Nonlinear transport

1. Introduction

A physical understanding of the adhesion between thermosets and thermoplastics has been obtained from previous studies [1–4]. These studies have shown that the load transfer at the dissimilar material interface can be dramatically improved when interdiffusion is possible. The graded interphase that is formed is believed to enhance bond strength through entanglements between the thermoplastic polymer chains and the network structure of the curing adhesive. A theoretical model for interdiffusion is needed to tailor the interphase size and properties during processing. One main factor that hinders a proper mathematical study of this phenomenon is that the diffusivity of the thermoset decreases with increasing reaction, due to increasing molecular weight. The phenomenological form of this diffusivity expression was determined in a previous work [5]. In addition, reaction depletes the concentration of the diffusing epoxy and amine monomers. The model developed in this study incorporates these two important mechanisms viz. effect of reaction on diffusivity and on concentration.

Recent studies by Rajagopalan et al. [1,4] have shown that a stoichiometric mixture of diglycidyl ether of bisphenol A (DGEBA) epoxy and *para*-amino cyclohexyl methane (PACM 20) amine will diffuse into and cure in the presence of amorphous polysulfone (PSU). Using the ATR-FTIR technique [1,3,4], two characteristic epoxy peak absorbances were monitored with time—the reactive epoxide band at 915 cm^{-1} and the nonreactive aromatic band at 1036 cm^{-1}. The 1036 band absorbance equilibrated to an asymptotic value, while the reactive band absorbance increased initially from diffusion, but subsequently decreased to values close to zero during reaction.

In a subsequent study [5], a phenomenological diffusivity model for the diffusion with reaction and swelling of DGEBA epoxy and PACM 20 amine monomers in amorphous PSU was developed. Parametric studies showed that the predicted diffusivity decreases significantly with increasing thermoset reaction.

Past work pertaining to the transport modeling of coupled diffusion-reaction phenomena in polymer systems is scarce. Using a constant penetrant diffusivity, Beenackers et al.

* Corresponding author. Tel.: + 1-302-831-8702; fax: + 1-302-831-8525.

E-mail address: gillespie@ccm.udel.edu (J.W. Gillespie Jr.).

0032-3861/00/$ - see front matter
PII: S0032-3861(00)00251-2

Nomenclature

a	Oscillator strength
A	Absorbance
B	Critical free volume size for diffusion
c_a^{norm}	Normalized amine concentration
c_e, c_a	Epoxy, amine concentration
c_{e0}, c_{a0}	Initial epoxy, amine concentration
D	Diffusivity
$D_{e(a)}$	Amine concentration-dependent epoxy diffusivity
D_e, D_a	Epoxy, amine diffusivity
d_p	Depth of penetration
E_x/E_m	Ratio of segmental mobilities of crosslinked to uncrosslinked monomer
f	Fractional free volume
f_g	Fractional free volume at the glass transition temperature
F_x/F_m	Ratio of lattice energies of crosslinked to uncrosslinked monomer
K_1, K_2, k_1, k_2	Reaction rate constants
l	Film thickness
M, M_w	Molecular weight
M_e	Entanglement molecular weight
R	Universal gas constant
R_r	Reaction rate
S	Cross-sectional area
T	Temperature
t	Time
T_g	Glass transition temperature
T_{g0}	Glass transition temperature of uncrosslinked monomer
x	Distance
α	Degree of cure
β	Thermal expansion coefficient
ε	Volume fraction of penetrant
γ	Swelling constant

developed a numerical model that describes non-Fickian diffusion with swelling and chemical reaction of a penetrant A with a reactive group B of a glassy polymer [6]. Subsequently they modified this model to accommodate consecutive and parallel reactions of the penetrant with the polymer and the reaction product [7]. Since the penetrant reacts with the polymer, this does not apply to our present case. Cunningham et al. developed a coupled diffusion-reaction model for the diffusion of oxygen coupled with oxidative and non-oxidative reactions in polymer matrix composites [8]. They used a single concentration dependent reaction coupled with a Fickian diffusion model using a constant diffusivity and implemented it using a one-dimensional explicit time-step finite difference code. The present situation is more complex. Here, the epoxy and amine monomers diffuse into amorphous PSU at varying rates, leading to two governing transport equations. This system of governing equations is expected to be strongly coupled from the dependence of the epoxy diffusivity on amine concentration, and through the reaction terms. Further the diffusivities of the epoxy and amine are also strong functions of cure.

In this study the influence of swelling and reaction on the epoxy and amine concentration is further captured through the formulation and development of a transport model. Specifically, a mathematical model for the diffusion of epoxy and amine with swelling and reaction in the amorphous polymer is developed to gain a fundamental understanding of the coupled diffusion-reaction-swelling process. Further, this model is used to predict the concentration profiles with time and distance in the epoxy–amine-PSU system. The model predictions are validated with experimental data from ATR-FTIR [1] and SEM-EDS studies from [9].

2. Models

2.1. Kinetic model for DGEBA epoxy-PACM amine cure

The cure kinetics model for this resin system was developed by Sanford [10]. The main results of this kinetic model that he developed are presented in this section. The

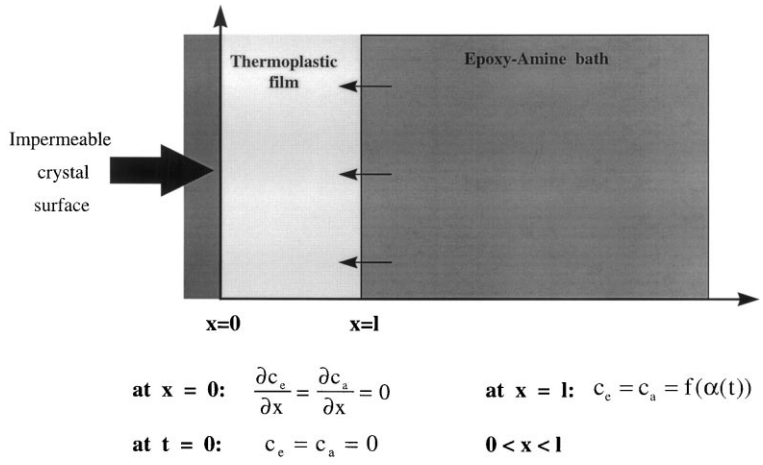

Fig. 1. Mathematical set-up for the diffusion of reacting epoxy–amine into amorphous thermoplastics.

rate of the cure reaction can be expressed as a function of time and temperature. The reaction between epoxies and amines is generally autocatalytic in nature, due to the formation of proton donors like the hydroxyl group. The form of the reaction rate equation used to describe these intrinsic kinetics is:

$$R_r = -\frac{dc_e}{dt} = (K_1 + K_2(c_{e0} - c_e))c_e c_a \quad (1)$$

where K_1 and K_2 have an Arrhenius temperature dependence, and are given as [4,10]:

$$K_1 = \frac{k_1}{c_{e0}c_{a0}} \quad (2)$$

$$K_2 = \frac{k_1}{c_{e0}^2 c_{a0}} \quad (3)$$

where:

$$k_1\ (s^{-1}) = 0.0 \quad (4)$$

$$k_2\ (s^{-1}) = 1.47 \times 10^5 \exp\left(-\frac{12\,022}{RT}\right) \quad (5)$$

The degree of cure, α, is given as:

$$1 - \alpha = \frac{c_e}{c_{e0}} = \frac{c_a}{c_{a0}} \quad (6)$$

which on insertion in Eq. (1) and discretizing, gives:

$$\alpha = \frac{(K_1 + K_2(c_{e0} - c_e))c_e c_a \Delta t}{c_{e0}} \quad (7)$$

In these equations "e" and "a" refer to epoxy and amine, respectively; c is the concentration, c_{e0} and c_{a0} are the initial epoxy and amine concentrations, α is the degree of cure, R is the universal gas constant (cal/mol K), T is the temperature, and t is the time.

2.2. Transport model

2.2.1. Formulation of the governing equations

The mathematical problem for this study is shown in Fig. 1 and reflects the experimental ATR-FTIR set-up examined previously [1–4]. The infrared crystal interface constitutes the impermeable boundary and gives rise to a no-flux condition at $x = 0$. Interdiffusion of epoxy and amine monomers occurs at the bath-film interface ($x = l$). The influence of the mechanisms of reaction and swelling on transport is intricate and can be studied in the framework of classical one-dimensional Fickian diffusion kinetics to obtain a preliminary understanding. The general governing equations for epoxy and amine transport in amorphous thermoplastics are given below:

$$\frac{\partial c_e(\alpha)}{\partial t} = \frac{\partial}{\partial x}\left(D_e(\alpha, c_a, \varepsilon)\frac{\partial c_e(\alpha)}{\partial x}\right) - R_r(\alpha) \quad (8)$$

$$\frac{\partial c_a(\alpha)}{\partial t} = \frac{\partial}{\partial x}\left(D_a(\alpha, \varepsilon)\frac{\partial c_a(\alpha)}{\partial x}\right) - R_r(\alpha) \quad (9)$$

where subscripts "e" and "a" are for epoxy and amine, respectively. The boundary condition at $x = l$ i.e. the bath-film interface, becomes:

$$c_e = c_{e0}(1 - \alpha) \quad (10)$$

$$c_a = c_{a0}(1 - \alpha) \quad (11)$$

where α is obtained from Eq. (7).

Further, the epoxy and amine diffusivity expressions are obtained from [5]:

$$\frac{D_e(\alpha, c_a, \varepsilon)}{D_{e(a)}(c_a, T)} = \exp\left(B\left(-\frac{s_1\alpha\varepsilon}{(f_{tp}^0(1-\varepsilon)(1-s_2\alpha) + (f_{ts}^0 - (f_{ts}^0 s_2 + s_1)\alpha)\varepsilon)(f_{tp}^0(1-\varepsilon) + f_{ts}^0\varepsilon)}\right)\right) \quad (12)$$

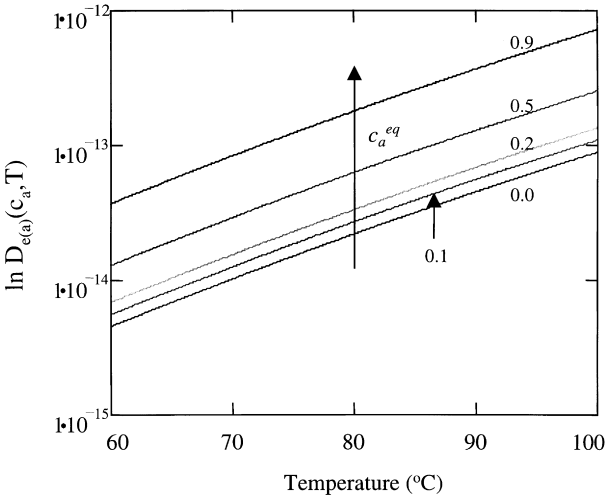

Fig. 2. Effect of amine concentration on epoxy diffusivity (Eq. (13)).

with:

$$D_{e(a)}(c_a, T)\ (m^2/s) = 52.3 \times 10^{-4} \exp(2.1 c_a^{norm}) \exp\left(-\frac{18\,500}{RT}\right) \quad (13)$$

Eq. (13) is the expression for increased epoxy diffusivity from swelling (Fig. 2 [4,5]). The corresponding expression for the amine is given by:

$$\frac{D_a(\alpha, \varepsilon)}{D_a(T)} = \exp\left(B\left(-\frac{s_1 \alpha \varepsilon}{(f_{tp}^0(1-\varepsilon)(1-s_2\alpha) + (f_{ts}^0 - (f_{ts}^0 s_2 + s_1)\alpha)\varepsilon)(f_{tp}^0(1-\varepsilon) + f_{ts}^0 \varepsilon)}\right)\right) \quad (14)$$

where ε is the total epoxy and amine concentration ($\varepsilon = c_a + c_e$), and:

$$D_a(T)\ (m^2/s) = 1.044 \times 10^{21} \exp\left(-\frac{54\,000}{RT}\right) \quad (15)$$

Table 1
Model inputs for the DGEBA-PACM-PSU material system

D_e (m^2/s)	$52.93 \times 10^{-4} \exp(-18\,500/RT)$
D_a (m^2/s)	$1.04 \times 10^{21} \exp(-54\,000/RT)$
k_1 (s^{-1})	0.0
k_2 (s^{-1})	$147 \times 10^3 \exp(-12\,022/RT)$
T_gPSU (°C)	191
T_{g0}	−20
B	1.1
c_{e0}	1
c_{a0}	1
F_g	0.025
E_x/E_m	0.337
F_x/F_m	0.194
β (°C^{-1})	4.08×10^{-4}
d_p (μm)	0.54 for 1036 cm^{-1}
	0.48 for 915 cm^{-1}

$$s_1 = \beta T_{g0}\left(\frac{E_x}{E_m} - \frac{F_x}{F_m}\right) \quad (16)$$

$$s_2 = 1 - \frac{F_x}{F_m} \quad (17)$$

$$f_{tp}^0 = f_{tp}(0, T) \quad (18)$$

$$f_{ts}^0 = f_{ts}(\alpha = 0, T) \quad (19)$$

In these equations β is the thermal expansion coefficient of free volume, T_{g0} is the glass transition temperature of the uncrosslinked monomer, E_x/E_m and F_x/F_m are the ratio of the segmental mobilities and lattice energies, respectively, of the crosslinked to uncrosslinked monomers, "ts" and "tp" refer to the thermoset and thermoplastic, respectively. The fractional free volume, f, is defined as [4,5]:

$$f = f_g + \beta(T - T_g) \quad (20)$$

Eqs. (8) and (9) are coupled through the swelling dependence of the epoxy diffusivity [5], and the reaction term, R_r, in Eq. (1). Hence they represent transport with interacting mechanisms of swelling and reaction on diffusion. Nonlinear Fickian transport can occur if the diffusion is concentration dependent.

In the present case, substitution of Eq. (1) for the reaction rates expression into Eqs. (8) and (9) yields the desired equations for transport for the epoxy and amine:

$$\frac{\partial c_e}{\partial t} = \frac{\partial}{\partial x}\left(D_e(\alpha, c_a, \varepsilon)\frac{\partial c_e(\alpha)}{\partial x}\right) - (K_1 + K_2(c_{e0} - c_e))c_e c_a \quad (21)$$

$$\frac{\partial c_a}{\partial t} = D_a(\alpha\varepsilon)\frac{\partial^2 c_a}{\partial x^2} - (K_1 + K_2(c_{e0} c_e))c_e c_a \quad (22)$$

where $D_e(\alpha, c_a, \varepsilon)$ is the cure and amine-concentration dependent epoxy diffusivity (Eq. (12)), and $D_a(\alpha, \varepsilon)$ is the cure dependent amine diffusivity (Eq. (14)) [5]. The governing Eqs. (21) and (22) are coupled and nonlinear in nature. Further, the diffusivities are time-dependent. These equations assume that the epoxy (or amine) diffusivity is unaffected by the epoxy to amine stoichiometric variation with distance, leading to the independence of diffusivity, D, with distance. For this epoxy–amine system, Skourlis [11] showed weak dependence of cure on stoichiometry until gelation, and Vanlandingham [12] showed that stoichiometric variations affect the diffusivity to a minor extent, thereby supporting this assumption.

The mathematical (and experimental) set-up with the

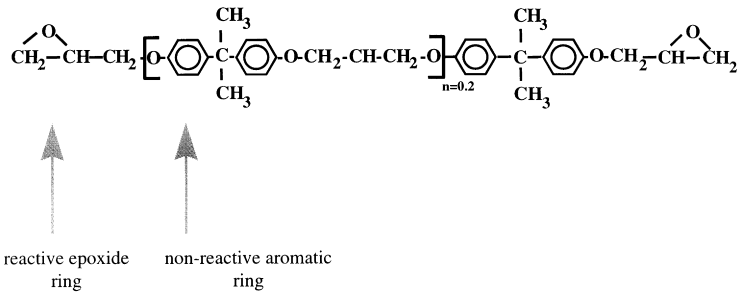

Fig. 3. Structure of the DGEBA epoxy molecule.

boundary and initial conditions are shown in Fig. 1 and are given as:

$$\frac{\partial c_e}{\partial x} = \frac{\partial c_a}{\partial x} = 0 \qquad \text{at } x = 0 \tag{23}$$

$$c_e = c_a = 0 \qquad \text{at } t = 0, 0 < x < l \tag{24}$$

where c is the concentration of the penetrant. The boundary condition at $x = l$ is given as:

$$\frac{dc_e}{dt} = -(K_1 + K_2(c_{e0} - c_e))c_e c_a \tag{25}$$

$$\frac{dc_a}{dt} = -(K_1 + K_2(c_{a0} - c_a))c_e c_a \tag{26}$$

The solution for the set of Eqs. (21)–(26) is obtained numerically using finite difference methods. The approach and development of this scheme is outlined in Appendix A.

2.3. Model inputs

For the DGEBA epoxy-PACM 20 amine-PSU material system, the inputs for the numerical model are as shown in Table 1. The Arrhenius diffusivity and reaction rate expressions determined in past work [1–3] are used here.

3. Results and discussion

In this section by using the epoxy and amine diffusivity expressions with the transport model developed for the system of Eqs. (21)–(26), the nature of the coupled diffusion-reaction process is examined. The concentration profiles predicted by the model are used as input into Eq. (27) to estimate data from the ATR-FTIR. The concentration profiles generated by the model can be converted to the ATR-FTIR absorbance, A, by the following equation, which is analogous to the Beer–Lambert law for absorption transmission infrared spectroscopy [1,3,4]:

$$A = \int_0^\infty aSC(x) \exp\left(-\frac{2x}{d_p}\right) dx \tag{27}$$

where x is the distance from the surface, a is the oscillator strength, $C(x)$ is the concentration of absorbing species, S is the cross-sectional area, and d_p is the penetration depth

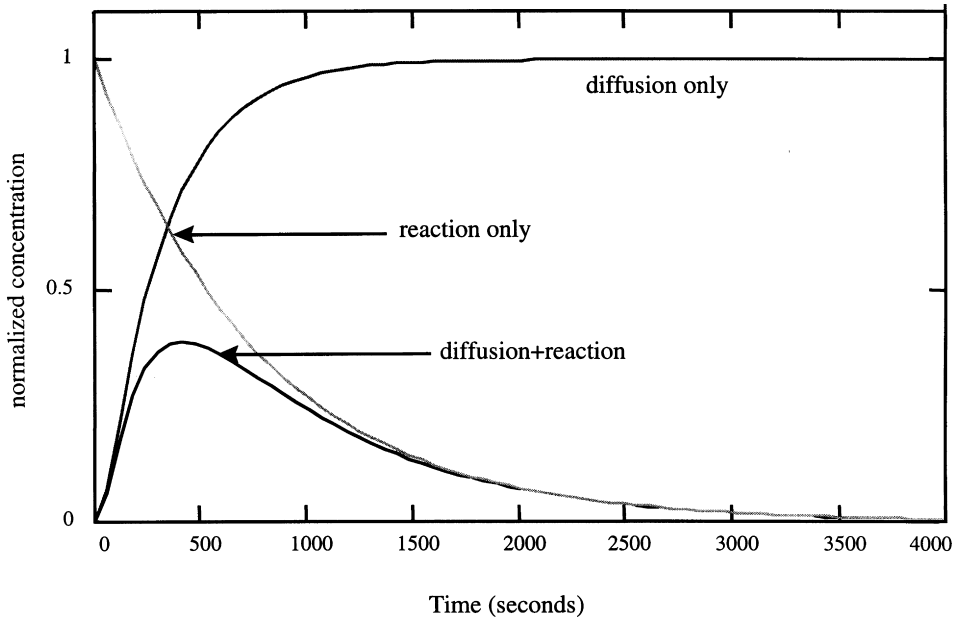

Fig. 4. Nature of the coupled diffusion-reaction process showing a superposition of the reaction process over diffusion.

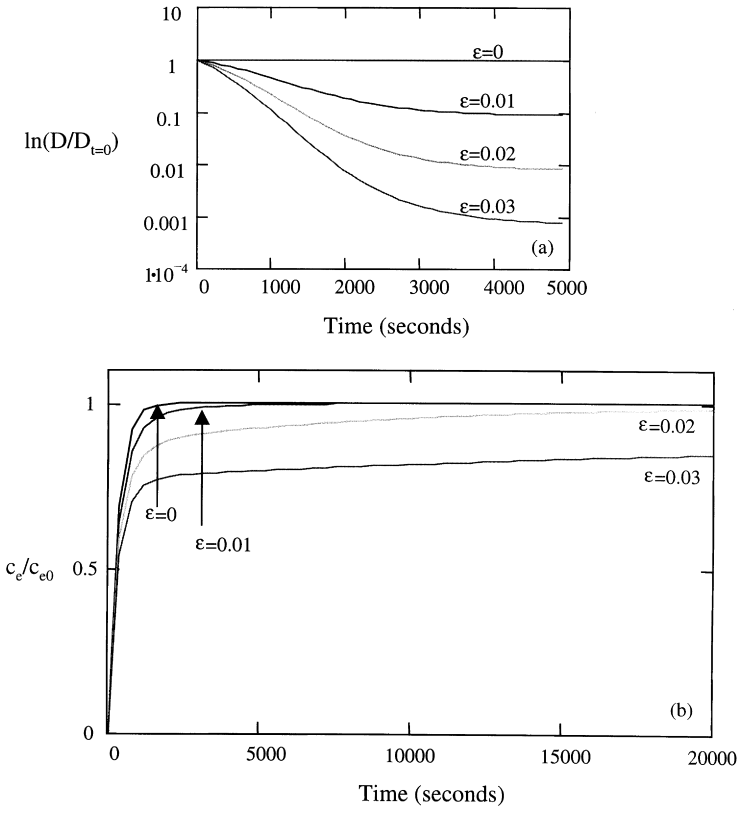

Fig. 5. Effect of % thermoset, ε, on (a) diffusivity and (b) normalized non-reactive epoxy peak concentration vs. time. $T = 80°C$, $B = 1$.

[3,4]. Thus, the absorbance at any time is related to the weighted average of the concentration as a function of position away from the IRE surface. By solving the appropriate diffusion equation for an ATR-FTIR experiment, the absorbance can be directly used to quantitatively evaluate diffusion processes. The following assumptions are implicit in the use of Eq. (27) viz (a) the penetration depth, d_p, is a constant for the band of interest; (b) the ratio of the film thickness to penetration depth, l/d_p, should always be greater than 5 for the analysis to be valid [13]; and (c) the refractive index of the polymer does not change with concentration or composition [13].

Next, model predictions for the absorbance profiles are compared to the ATR-FTIR data [1]. The spatial concentration profiles are used to predict the interphase sizes in this material system as a function of time. These predictions are validated with experimental AFM and SEM-EDS results on interphase size from Immordino's work [3,9].

3.1. Generic nature of a diffusion-reaction process

The structure of the epoxy molecule is shown in Fig. 3. The reactive group is the epoxide ring, while the aromatic groups attached to this ring constitute the non-reactive groups that do not partake in the reaction. As diffusion occurs, the absorbance of the reactive peak (A_R) is affected by diffusion, and tends to increase. Reaction tends to decrease A_R with time. Hence A_R will show an initial increase from diffusion and a final decrease from reaction. With continuing reaction, the epoxy chain molecular weight increases. This effect is evident in the absorbance of the non-reactive groups (A_{NR}) that are only affected by reaction effects on diffusion. Therefore A_{NR} shows an increase towards an equilibrium value, at a slower rate than for a diffusion-only situation. At complete conversion, A_R goes to zero, and the epoxy chains are crosslinked and branched and diffusion ceases at this point. Observing A_{NR} gives the equilibrium amount of epoxy monomers that have diffused in and reacted, and it can be used to compute the relative amounts of epoxy, amine, and PSU in the ternary mixture.

Fig. 4 shows the general nature of the coupled diffusion-reaction process, along with curves for diffusion-only and reaction-only. In a diffusion-only process, the penetrant diffuses in without hindrances to mobility (i.e. changes to the chain molecular weight) e.g. solvent diffusion into polymers, and the single component diffusion of epoxy or amine monomers into polymers [2,3]. A reaction-only process involves a consumption of reactive groups only, without large-scale diffusive motion across a physical interface. Such a process is commonly observed during cure in bulk thermosets [10], where epoxide and amine hydrogen groups are consumed with time. Hence, it is clearly seen that the coupled process is a superposition of these two individual processes. Further, diffusion appears to be the dominant mechanism initially, with reaction dominating at later

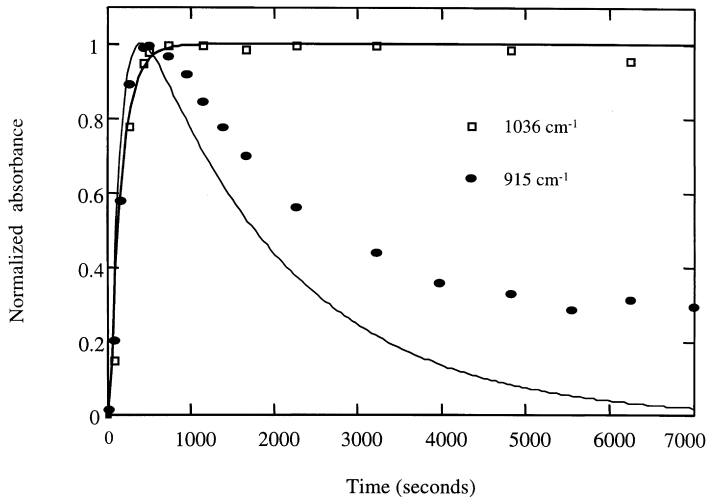

Fig. 6. Model predictions compared to experimental data of normalized absorbance vs. time at 60°C for the reacting 915 cm^{-1} epoxide ring, and the non-reacting 1036 cm^{-1} aromatic ring. Film thickness = 1.5 μm.

stages. These results show qualitative agreement with the experimental findings reported in Rajagopalan et al. [1].

Fig. 5(a) describes the variation of epoxy diffusivity with time for increasing volume fraction of the thermoset, ε, seen previously [5], with the resulting effects on A_{NR} vs. ε shown in Fig. 5(b). These studies show that small changes in ε affect normalized epoxy concentration profiles considerably. With increasing values of ε, the diffusion process is further retarded, and the equilibrium concentration is approached more slowly. The reason for this predicted behavior is that with increasing amounts of thermoset, the effects of reaction on the fractional free volume are more prominent, and the initially rapid diffusion is slowed down from the growing molecular weight of the diffusing thermoset.

For model predictions and validation the absorbance and spatial concentration distributions of the epoxy peaks are studied, as the epoxy monomer has the lower diffusivity and will show more prominent effects of reaction on diffusion. It will also control the size of the interphase.

3.2. Absorbance vs. time

This section describes the model predictions corresponding to the experimental ATR-FTIR results from [1], where the diffusion with reaction and swelling of a stoichiometric amount of epoxy–amine mixture (75:25 vol.%) into amorphous PSU was studied.

3.2.1. Non-reacting peak

The non-reactive epoxy (or amine) peaks are not involved in the epoxy–amine reaction and are not consumed. They, however, reflect changes from reaction effects (i.e. increasing molecular weight) on diffusivity. Some non-reactive

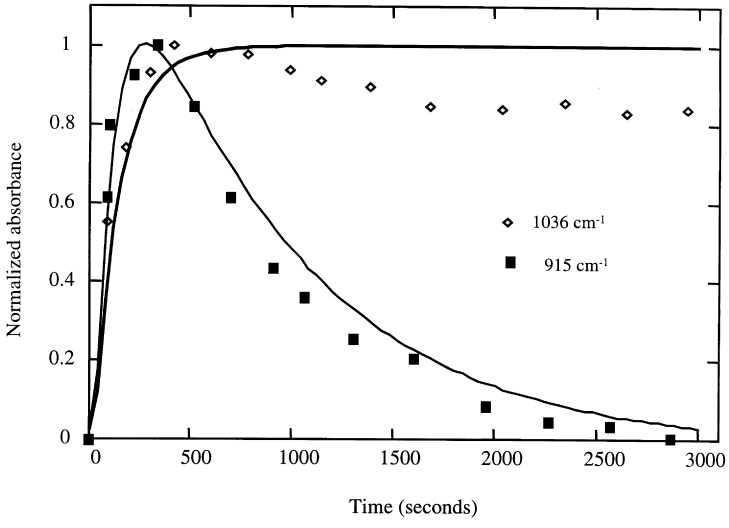

Fig. 7. Model predictions compared to experimental data of normalized absorbance vs. time at 80°C for the reacting 915 cm^{-1} epoxide ring, and the non-reacting 1036 cm^{-1} aromatic ring. Film thickness = 4 μm.

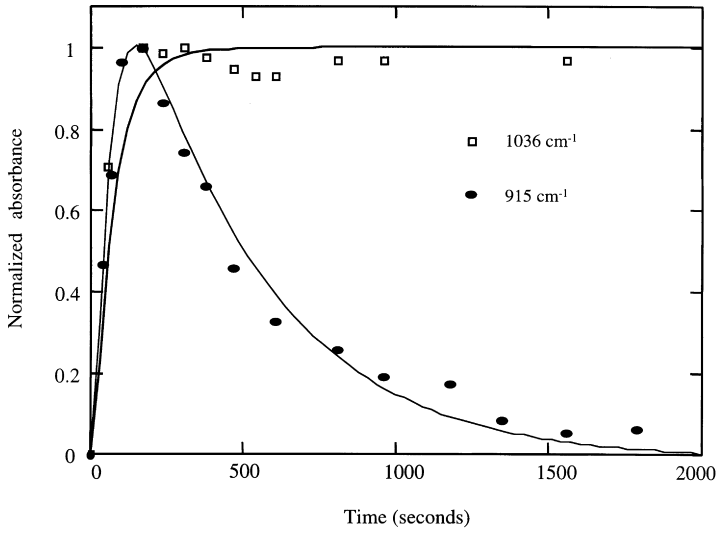

Fig. 8. Model predictions compared to experimental data of normalized absorbance vs. time at 90°C for the reacting 915 cm^{-1} epoxide ring, and the non-reacting 1036 cm^{-1} aromatic ring. Film thickness = 4 μm.

peaks include the DGEBA peak (1036 cm^{-1}) and PACM amine peak (2916 cm^{-1}) [1,3,4].

The model predictions for the non-reactive 1036 cm^{-1} epoxy peak at the temperatures studied are shown in Figs. 6–8. Model predictions are satisfactory at 60°C; however, some predictions deviate from experimental data at the higher temperatures. Swelling is the cause for the observed deviations in the experimental data at higher temperatures. These predictions suggest that the assumptions inherent in this model are adequate to determine the behavior of the non-reacting group with time.

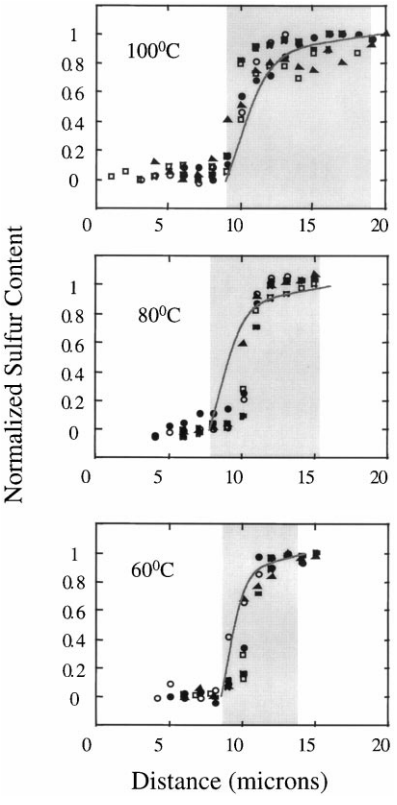

Fig. 9. SEM-EDS experimental data (●, ○, ▲, □, ■) [9] with model predictions (solid line). Gray areas show the approximate interphase size.

3.2.2. Reacting species

The predictions of the numerical model for the normalized reactive peak absorbance vs. time are shown in Figs. 6–8. These predictions are quite accurate at 80 and 90°C, while deviations are seen at 60°C, though the trend is predicted well. Further, the epoxy–amine reaction does not go to completion at this temperature, which is not captured by the model since bulk epoxy–amine diffusion limitations on reaction are not accounted for in the model development. The occurrence of the peak maximum is predicted very accurately at these temperatures, suggesting that the epoxy–amine reaction rate for cure in the presence of PSU is quite similar to the bulk cure kinetics and is not altered significantly. Additionally it also suggests that the diffusivity and transport model capture well the effects of reaction on monomer diffusivity and concentration. These correlations serve to validate these models.

3.3. Concentration vs. distance

These predictions on the epoxy concentration are used to determine the interphase size in this material system. The experimental SEM-EDS results on the size of the interphase formed during the diffusion of a stoichiometric amount of epoxy and amine into amorphous PSU [3,9] are shown in Fig. 9. The EDS results are obtained by tracing sulfur present in the PSU across the epoxy–amine-PSU interface.

The predictions of the numerical model for the diffusion and subsequent reaction, with amine swelling, of DGEBA

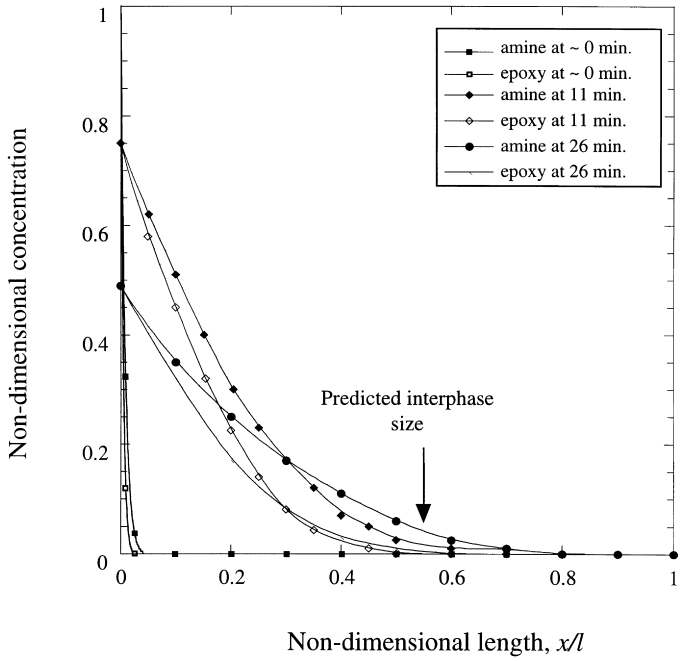

Fig. 10. Non-dimensional concentration profiles for epoxy and amine as a function of distance at 60°C. Swelling is assumed to enhance the epoxy diffusivity. Film thickness = 10 μm.

epoxy and PACM 20 amine monomers in the temperature range 60 to 100°C are given in Figs. 10–12. The diffusion of the epoxy monomers ceases beyond certain times, and these times are defined as the diffusion cessation times. Negligible increments in the interphase size are obtained for greater processing times. In this study, the interphase size is defined as the distance at which the epoxy concentration at the diffusion cessation time drops to 1% of the initial value. Using this definition, correlations between the predictions and data can be made.

Fig. 9 shows the model predictions with the experimental EDS results [9] at 60, 80 and 100°C. The normalized model

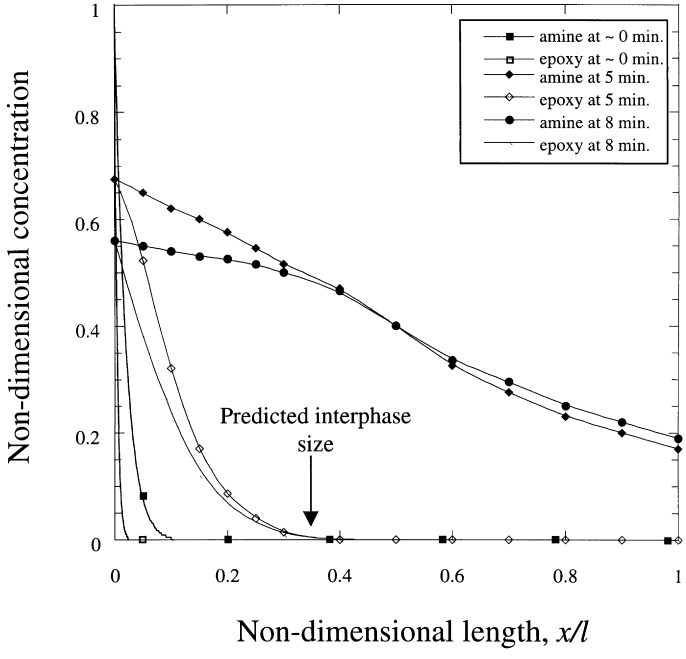

Fig. 11. Non-dimensional concentration profiles for epoxy and amine as a function of distance at 80°C. Swelling is assumed to enhance the epoxy diffusivity. Film thickness = 20 μm.

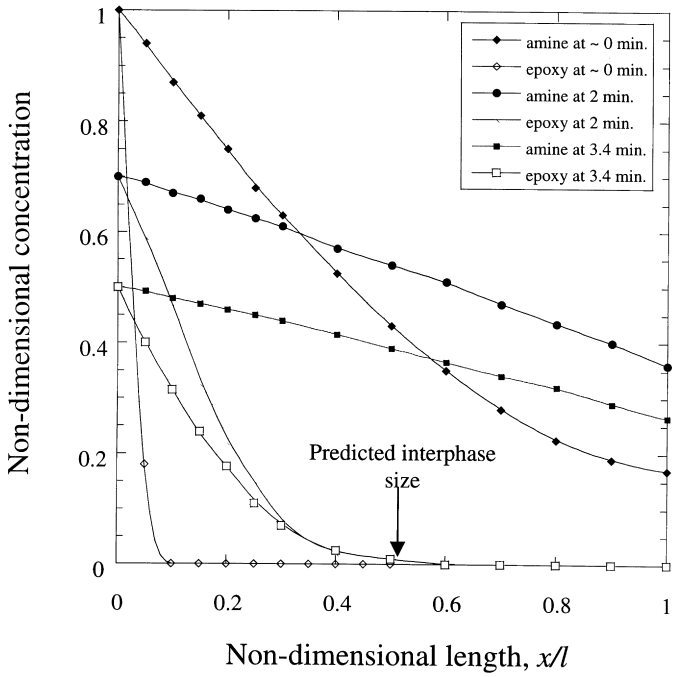

Fig. 12. Non-dimensional concentration profiles for epoxy and amine as a function of distance at 100°C. Swelling is assumed to enhance the epoxy diffusivity. Film thickness = 20 μm.

predictions are obtained using the following expression:

$$c_{PSU} = 1 - c_e - c_a \quad (28)$$

It is seen that the model predicts very accurately the interphase size in these material systems. Further the effect of the mechanisms of reaction and swelling on interphase predictions can be understood by incorporating each mechanism incrementally and studying the resulting changes in the predictions on interphase size. Table 2 provides a summary of the various intermediate models developed in this work and the evolution in their predictions. When thermoset diffusivity is considered constant, i.e. without swelling or reaction effects ($\alpha = 0$, $c_a^{norm} = 0$ in Eqs. (12) and (13), respectively), it is seen that the model overpredicts interphase size at the diffusion cessation time for all temperatures. By including reaction effects on diffusivity without swelling effects ($c_a^{norm} = 0$ in Eq. (13)), the model gives realistic estimates on the interphase size, suggesting that reaction effects on diffusivity and concentration are crucial in making accurate predictions on the growth of the interphase with processing conditions. Finally, by incorporating the swelling contributions to the diffusivity, a slight increase in predicted interphase size is seen at the higher temperatures. The predictions of the reaction-only and reaction and swelling models fall within the experimental range of interphase values at each temperature, and this suggests that swelling may play a minor role in controlling the interphase size in this system. Hence, this result justifies the Fickian approach to problem formulation used here, without the consideration of moving boundaries and density variations. The reaction-swelling model can prove beneficial for the study of interphase formation in systems where swelling may play a major role, in addition to reaction, e.g. diffusion of amine-rich resins into amorphous polymers where a greater amount of swelling is possible, thereby increasing epoxy diffusivity and the interphase size.

A consequence of different epoxy and amine diffusivities at the higher temperatures is the development of stoichiometric gradients along the film. Several researchers have concluded that deviations from an optimum stoichiometry will lead to a loss in macroscopic thermoset properties [13,14]. For this system, this effect will be small for films

Table 2
Interphase size predictions at diffusion cessation times from the models developed in this work vs. experimental data. Sizes are defined at 1% of initial epoxy concentration

Temperature (°C)	Experimental		Diffusion only (no reaction, swelling)	Diffusion and reaction; no swelling	Diffusion, reaction, swelling
	EDS	AFM			
60	3–5	3	8	4	5
80	5–7	7	17	7	8
100	10–12	12	20	10	11

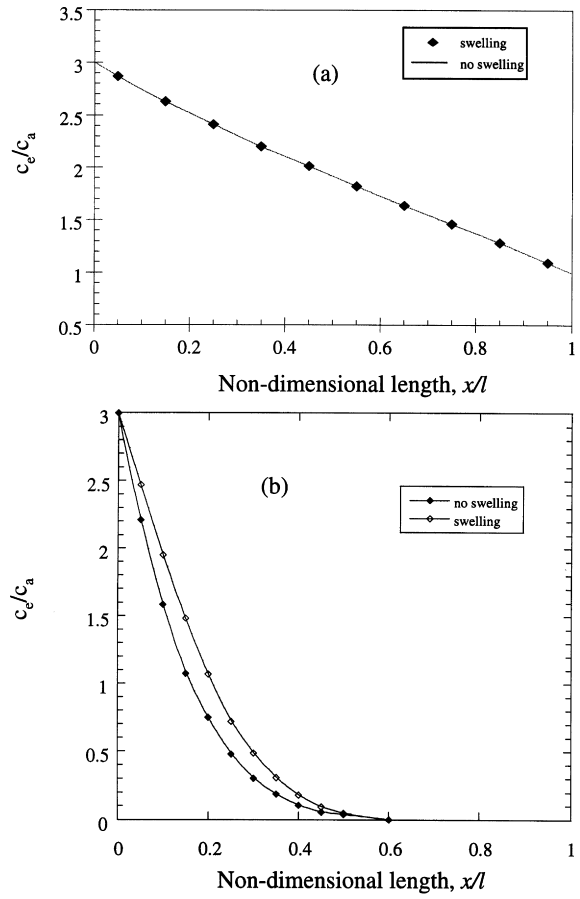

Fig. 13. Development of stoichiometric gradients for epoxy–amine diffusion-reaction in amorphous PSU at $t = t_{gel}$ (Table 3 [10]) at 100°C. (a) $l = 4$ μm, (b) $l = 20$ μm.

a few microns thick (3–4 μm), but not for films that are on the order of the interphase size at these temperatures (10–12 μm) (see Fig. 13). Further, swelling can lead to less steep stoichiometric gradients (Fig. 13) through an increase in epoxy diffusivity. As stoichiometry changes along the film, the properties of the crosslinked product formed will change, leading to differences in physical and mechanical properties along the interphase region. In this regard, other ways of defining the interphase size, based on the changing stoichiometry, may be required.

3.4. Reaction-limited diffusion

Diffusion ceases from reaction with time. The occurrence of this cessation is termed the diffusion cessation time and can be ascertained by studies on the spatial epoxy concentration distribution. As mentioned previously, this is defined as the time at which no further increases in the interphase size occur. Such times are identified as those corresponding to the epoxy concentration curves marked as "predicted interphase size" in Figs. 10–12. This way of representing the diffusion cessation point is a more consistent and dependable way than that described in previous studies [1,4] where the maximum in the reactive epoxide peak absorbance was used to define the time to diffusion cessation during interdiffusion. Table 3 gives a comparison of such points with the gelation times given by Sanford for the intrinsic epoxy–amine cure [1,4,10]. It is seen that maximum diffusive gains are achieved at far shorter times than the gel time determined for the intrinsic epoxy–amine cure. This implies that the reaction limits diffusion and, therefore, interphase formation at much lower conversions than that corresponding to the theoretical gel point ($\alpha = 0.63$). This is consistent with previous results [1,4].

Table 3
Diffusion cessation vs. temperature for the epoxy–amine-PSU system

Temperature (°C)	Diffusion cessation times from spatial epoxy concentration (s)	Get time (s) [10]
60	550	2200
80	300	770
100	120	330

4. Conclusions

This work has established a numerical model for the coupled diffusion-swelling-reaction phenomena observed in the DGEBA epoxy-PACM amine-PSU system, where two coupled, nonlinear equations of transport—one each for epoxy and amine—are required. Further by incorporating the phenomenological diffusivity model determined previously [5], the diffusivity model and the model predictions were successfully validated with the experimental results from previous studies [1,3,4,9].

The predictions of the transport model were validated using the ATR-FTIR experimental results on diffusion and reaction [1,4] and from interphase size data [3,4,9]. It is seen that the model predictions are accurate for the reactive and satisfactory for the non-reactive epoxy peak absorbances. Discounting swelling effects on thermoplastic density may be a reason for the deviation of model predictions from the non-reactive epoxy peak data. The model predictions on the reactive epoxy peak absorbance are precise, displaying the trend of initial diffusion with subsequent reaction seen experimentally. Further the temporal positions of the curve maximums are also well predicted. These points are indicative of when diffusion shuts down from reaction. This is a significant result, as it confirms that the model assumptions are representative of the diffusion-reaction behavior of the material system. Diffusional limitations on reaction build in beyond the gel point, and it is not expected that significant diffusion of the oligomers occurs beyond this point. Hence from a processing aspect, where maximum diffusion is required to get a large interphase, diffusion limitations need not be considered. The model also predicts that reaction limits interdiffusion of the epoxy–amine monomers at much earlier times than those

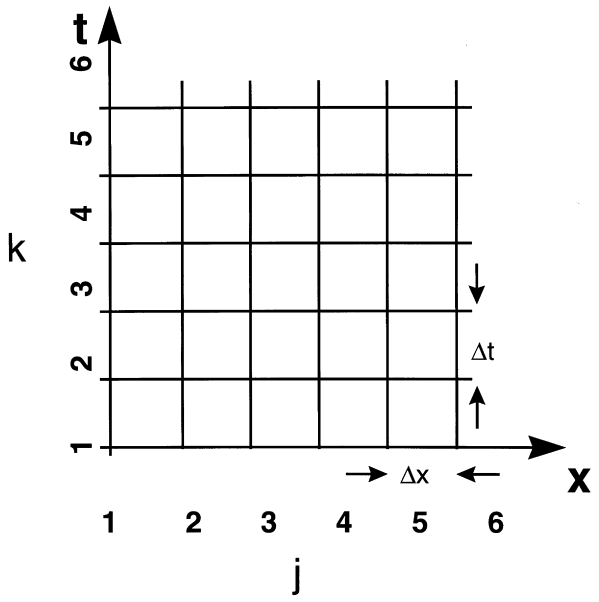

Fig. 14. Node set-up and discretization for finite difference approach for numerical modeling of coupled nonlinear diffusion-reaction equations.

given by Sanford for intrinsic thermoset cure, confirming results determined previously [1,4]. Additionally, the model predictions show that the assumption of an intrinsic reaction rate for the epoxy–amine in the presence of PSU is valid, as was previously determined [1,3,4].

It appears that pre-gelation processes and time scales are sufficient to predict the spatial and temporal distributions of concentration. Diffusion beyond the gel point is extremely difficult due to the high degree of crosslinking and the presence of thermoplastic chains; therefore, no significant changes in the interphase size are possible. The predictions at 80 and 100°C for the amine concentration reveal that the amine diffuses completely through the 20 μm thick thermoplastic film. This result seems to contradict the experimental ATR-FTIR findings, where no significant changes in the amine absorbance peak at 2916 cm^{-1} with time were observed for the larger films. While the plots show the normalized concentration distribution, it is believed that the amine concentration may be at amounts beyond the detectable range of the FTIR instrument (resolution = 4 cm^{-1}).

The following suggestions can be made for future work: in the study of the coupled diffusion-reaction phenomenon, it was shown that the epoxy–amine stoichiometry varies over the interphase region (Fig. 13). To determine the effects of these changes in composition on the properties of the interphase, the behavior of the ternary system has to be studied. Preparing blends of epoxy–amine-PSU at varying compositions and characterizing their microstructure and mechanical properties can facilitate this. Then the nature of the interphase can be inferred by mapping compositions predicted by the model to the experimentally determined properties.

Acknowledgements

This work was supported by the Composites Materials Research Collaborative Program sponsored by the US Army Research Laboratory under Cooperative Agreement DAAL01-96-2-0048.

Appendix A. Finite difference schemes for computation

The purpose of this section is to develop a simple and efficient computational technique that may be employed to produce numerical results of mathematical models of a chemical system in which chaotic behavior is not inherent. This technique was developed by Crank and Nicholson and is employed here to study the system of partial differential Eqs. (21)–(26) representing the diffusion, swelling, and reaction of an epoxy–amine system into an amorphous thermoplastic. The method is second order accurate in space and first order in time. This implicit method has enjoyed considerable success in solving nonlinear PDEs. The finite difference scheme is solved implicitly as a tridiagonal system using the Todd algorithm [15]. A similar algorithm is described in Wu and Peppas [16].

The initial/boundary-value problem is solved using finite difference methods by discretizing the space interval $0 < x < l$ into 1500 subintervals, each of width Δx, and by discretizing the time interval $t \geq 0$ into $l/1500$, where l is the film thickness (Fig. 14). The notations $c^e(j,k)$ for the epoxy and $c^a(j,k)$ for the amine will be used for the solution of the approximating finite difference method.

Finite difference equations are developed by approximating the time derivative in Eqs. (21) and (22) by the first order forward difference replacement:

$$\frac{\partial c^e(x,t)}{\partial t} = \frac{c^e(x,t+\Delta t) - c^e(x,t)}{\Delta t} \tag{A1}$$

Using our notation, this equation is

$$\frac{\partial c^e(j,k)}{\partial t} = \frac{c^e(j,k+1) - c^e(j,k)}{\Delta t} \tag{A2}$$

The space derivative is given as:

$$\frac{\partial c^e(x,t)}{\partial x} = \frac{c^e(x+\Delta x,t) - c^e(x,t)}{\Delta x} \tag{A3}$$

and in our notation:

$$\frac{\partial c^e(j,k)}{\partial x} = \frac{c^e(j+1,k) - c^e(j,k)}{\Delta x} \tag{A4}$$

Similarly, the second order space derivative is:

$$\frac{\partial^2 c^e(j,k)}{\partial x^2} = \left(\frac{D^e}{\Delta x^2}\right)[c^e(j-1,k+1) - 2c^e(j,k+1) + c^e(j+1,k+1) + c^e(j-1,k) - 2c^e(j,k) + c^e(j+1,k)] \quad \text{(A5)}$$

Similar expressions are used for the amine. These expressions, with the corresponding diffusivity expressions, can be inserted into the governing Eqs. (21) and (22) for the epoxy and amine, which are now written as:

$$\frac{\partial c^e(j,k)}{\partial t} = D_e(\alpha,\varepsilon)\gamma \exp(\gamma c^a(j,k))\left(\frac{\partial c^e(j,k)}{\partial x}\right)\left(\frac{\partial c^a(j,k)}{\partial x}\right) + D_e(\alpha,\varepsilon)\exp(\gamma c^a(j,k))\left(\frac{\partial^2 c^e(j,k)}{\partial x^2}\right) - (K_1 + K_2(c_{e0} - c^e(j,k)))c^e(j,k)c^a(j,k) + D_e(\alpha,\varepsilon)\frac{Bg_1(-g_2 f_{tp}^0 + \varepsilon^2(g_2 - g_3)(f_{tp}^0 - f_{ts}^0))}{(g_2(1-\varepsilon) + 2g_3\varepsilon)^2(f_{tp}^0(1-\varepsilon) + f_{ts}^0)^2} \times \exp(\gamma c^a(j,k))\left[\left(\frac{\partial c^e(j,k)}{\partial x}\right)^2 + \left(\frac{\partial c^e(j,k)}{\partial x}\right)\left(\frac{\partial c^a(j,k)}{\partial x}\right)\right] \quad \text{(A6)}$$

and:

$$\frac{\partial c^a(j,k)}{\partial t} = D_a(\alpha,\varepsilon)\left(\frac{\partial^2 c^a(j,k)}{\partial x^2}\right) - (K_1 + K_2(c_{a0} - c^a(j,k)))c^e(j,k)c^a(j,k) + D_a(\alpha,\varepsilon)\frac{Bg_1(-g_2 f_{tp}^0 + \varepsilon^2(g_2 - g_3)(f_{tp}^0 - f_{ts}^0))}{(g_2(1-\varepsilon) + 2g_3\varepsilon)^2(f_{tp}^0(1-\varepsilon) + f_{ts}^0)^2} \times\left[\left(\frac{\partial c^a(j,k)}{\partial x}\right)^2 + \left(\frac{\partial c^e(j,k)}{\partial x}\right)\left(\frac{\partial c^a(j,k)}{\partial x}\right)\right] \quad \text{(A7)}$$

where:

$$\gamma = 2.1 \quad \text{(A8)}$$

$$\varepsilon = c^a(j,k) + c^e(j,k) \quad \text{(A9)}$$

$$g_1 = s_1\alpha \quad \text{(A10)}$$

$$g_2 = f_{tp}^0(1 - s_2\alpha) \quad \text{(A11)}$$

$$g_3 = f_{ts}^0 - (f_{ts}^0 s_2 + s_1)\alpha \quad \text{(A12)}$$

Due to the amine-concentration dependence of the epoxy diffusivity, additional terms appear for the finite difference equations for the epoxy. The final set of equations, after simplification, is written as:

$$\beta_e c^e_{j+1,k+1} - (1 + 2\beta_e)c^e_{j,k+1} + \beta_e c^e_{j-1,k+1} = K_2(c_{e0} - c^e_{j,k})c^e_{j,k}c^a_{j,k}\Delta t - \frac{\beta_e}{2}D_e'(\alpha,\varepsilon)[c^e_{j+1,k} - c^e_{j-1,k}]^2 - \beta_e[c^e_{j+1,k} - 2c^e_{j,k} + c^e_{j-1,k}] + 2\beta_e D_e'(\alpha,\varepsilon)[(c^e_{j+1,k} - c^e_{j,k})(c^a_{j+1,k} - c^a_{j,k})] + \gamma\beta_e(c^e_{j+1,k} - c^e_{j,k})(c^a_{j+1,k} - c^a_{j,k}) \quad \text{(A13)}$$

for the epoxy, and:

$$\beta_a c^a_{j+1,k+1} - (1 + 2\beta_a)c^a_{j,k+1} + \beta_a c^a_{j-1,k+1} = \Delta t K_2(c_{e0} - c^e_{j,k})c^e_{j,k}c^a_{j,k} - \beta_a[c^a_{j+1,k} - 2c^a_{j,k} + c^a_{j-1,k}] - \frac{\beta_a}{2}D_a'(\alpha,\varepsilon)[c^a_{j+1,k} - c^a_{j-1,k}]^2 + 2\beta_a D_a'(\alpha,\varepsilon) \times[(c^e_{j+1,k} - c^e_{j,k})(c^a_{j+1,k} - c^a_{j,k})] \quad \text{(A14)}$$

for the amine, where:

$$\frac{D_e'}{D_e(\alpha,\varepsilon)} = \frac{D_a'}{D_a(\alpha,\varepsilon)} = \frac{Bg_1(-g_2 f_{tp}^0 + \varepsilon^2(g_2 - g_3)(f_{tp}^0 - f_{ts}^0))}{(g_2(1-\varepsilon) + 2g_3\varepsilon)^2(f_{tp}^0(1-\varepsilon) + f_{ts}^0)^2} \quad \text{(A15)}$$

$$\beta_e = \frac{D_e(\alpha,\varepsilon)\Delta t}{2\Delta x^2}\exp(\gamma c^a_{j,k}) \quad \text{(A16)}$$

$$\beta_a = \frac{D_a(\alpha,\varepsilon)\Delta t}{2\Delta x^2} \quad \text{(A17)}$$

The boundary conditions corresponding to Eqs. (25) and (26) are:

$$c^e_{j,k+1} = c^e_{j,k} - (K_1 + K_2(c_{e0} - c^e_{j,k}))c^e_{j,k}c^a_{j,k}\Delta t \quad \text{(A18)}$$

$$c^a_{j,k+1} = c^a_{j,k} - (K_1 + K_2(c_{a0} - c^a_{j,k}))c^e_{j,k}c^a_{j,k}\Delta t \quad \text{(A19)}$$

Eqs. (A13) and (A14) constitute the tridiagonal form, and an iterative method is used to solve the above equations. The details of this method of solution are found in Ref. [15].

A1. Criterion for stability

Stability for the tridiagonal system is defined as:

$$|1 + 2\beta_e| \geq |\beta_e| + |\beta_e| \quad \text{(A20)}$$

A similar expression for the amine is used. The stability criterion in Eq. (A20) is always true; hence the tridiagonal system always converges. This was ensured by choosing the values for the parameter space viz Δx and Δt so that the numerical scheme was stable and accurate.

References

[1] Rajagopalan G, Immordino KM, McKnight SH, Gillespie Jr. JW. Polymer 2000;41:2591.

[2] Immordino KM, McKnight SH, Gillespie Jr. JW. J Adhes 1998;65:115.

[3] Immordino KM. Characterization of the polysulfone/epoxy interphase for bonding thermoplastic composites, MS Thesis, University of Delaware, Newark, DE, 1996.

[4] Rajagopalan G. Diffusion of reacting thermosets into thermoplastics, PhD Dissertation, University of Delaware, DE, 1999.

[5] Rajagopalan G, McKnight SH, Gillepsie JW Jr. Submitted for review.

[6] Kuipers NJM, Beenackers AACM. Chem Engng Sci 1993;48:2957.

[7] Kuipers NJM, Beenackers AACM. Polym Engng Sci 1996;36:2108.

[8] Cunningham RA, McManus HL. Proc ASME Aerospace Division 1996;52:353.

[9] Rajagopalan G, Immordino KM, McKnight SH, Gillespie JW Jr. Proceedings of the 11th Technical Conference of the American Society for Composites, 539, 1996.

[10] Sanford WM. Cure behavior of thermosetting resin composites, PhD Dissertation, University of Delaware, Newark, DE, 1987.

[11] Skourlis TP. Structure and properties of the interphase in coated carbon fiber epoxy systems, PhD Dissertation, University of Delaware, Newark, DE, 1995.

[12] Vanlandingham MR. Characterization of interphase regions in fiber-reinforced polymer composite materials, PhD Dissertation, University of Delaware, DE, 1998.

[13] Skourlis TP, McCullough RL. J Appl Polym Sci 1994;52:1241.

[14] Palmese GR. Origin and influence of interphase material property gradients in thermosetting composites, PhD Dissertation, Department of Chemical Engineering, University of Delaware, Newark, DE, 1991.

[15] Todd J. Survey of numerical analysis. New York: McGraw-Hill, 1962.

[16] Wu JC, Peppas NA. J Appl Polym Sci 1991;49:1845.